NUMERICAL SIMULATION ON THE EMISSION OF NO_x FROM THE COMBUSTION OF NATURAL GAS IN THE SIDEWALL BURNER

by

***Mingyu WANG** [a], **Jing ZHAO** [a], **Feihong GUO** [b], **Lingli ZHU** [a], **Dekui SHEN** [a*], and **Xiaoxiang JIANG** [b*]*

[a] Key Laboratory of Energy Thermal Conversion and Control of Ministry of Education, School of Energy and Environment, Southeast University, Nanjing, Jiangsu, China
[b] Engineering Laboratory of Energy System Process Conversion and Emission Reduction Technology of Jiangsu Province, School of Energy and Mechanical Engineering, Nanjing Normal University, Nanjing, Jiangsu, China

Original scientific paper
https://doi.org/10.2298/TSCI200916061W

The NO_x produced from industrial facilities is a serious environmental problem in China. In this work, the NO_x emission from the combustion of natural gas in the sidewall burner was investigated by using CFD method. To achieve the low NO_x emission, the sidewall burner structure was optimized involving the width of the primary premixed gas outlet, the secondary fuel gas nozzles number and angular spacing. The mixing rate of fuel gas and air could be improved by increasing the width of primary premixed gas outlet, and the lowest NO_x emission of 32.8 ppm was achieved at the width of 8 mm. The NO_x emission was remarkably reduced with the increasing of nozzles number, where 28.33 ppm of NO_x emission and 357.35 ppm of CO were obtained at four nozzles. The combustion performance and NO_x emission was improved as well as NO_x emission was reduced at the angular spacing of 55°, compared to that of 30°, 35°, 40°, 45°, 50°, and 60°.

Key words*: NO_x, combustion performance, numerical simulation, burner structure, fuel gas*

Introduction

Nitrogen oxides are one of the main atmospheric pollutants, which could cause acid rain and photochemical smog [1, 2]. Gaseous fuels have been widely used to meet the stringent emission requirements [3]. Although the combustion of gaseous fuels can greatly reduce the emission of solid particulate matters and sulfur oxides, the NO_x emission is still a problem that needs to be solved.

Nowadays, many efforts have been done to reduce the emission of NO_x by optimizing operating parameters. It has been reported that the NO_x emission could be reduced by optimizing excess air ratios and staged air-flow percentage [4]. Li *et al.* [5] studied the NO_x emission characteristics at different loads, and investigated the combustion and NO_x emission characteristics of real combustors. Lee *et al.* [6] investigated the effect of fuel distribution ratio on NO_x emission and found that the increased distribution ratio would benefit reducing NO_x emission. Nevertheless, reducing NO_x emission by changing the operating parameters was limited and would lead to a poor combustion performance.

* Corresponding author, e-mail: 101011398@seu.edu.cn, 62081@njnu.edu.cn

Reducing NO_x emission by optimizing the arrangement of burners or the structure of a single burner is another efficient way [7]. Nhan *et al.* [8] designed a newly flue-gas internal re-circulation burner, which may greatly diminish NO_x emission. Chen *et al.* [9] designed a burner structure which could form the folded flame, and the results showed that the moderated burner was a benefit in reducing NO_x emission and improving combustion performance. Iyogun *et al.* [10] changed the nozzle geometry and swirl intensity to obtain the optimal combustion condition. Fan *et al.* [11] investigated the effect of the distance between fire and sidewall by experiment and found that by changing the term pool, the more intense combustion was acquired. However, due to the limitation of measurement technologies and experimental conditions, the details of combustion cannot be observed in the experiment.

Recently, with the development of computing power and methodology, CFD calculations became a popular research method for burner structure optimization, which presented more details in the combustion process. It was reported that the combustion performance could be evaluated by the CO contribution condition and the temperature fields by CFD calculation [12-14]. Besides, NO_x emission was another important index to evaluate the burner performance [15]

In this study, the single low NO_x sidewall burner model was established by SOLIDWORKS and evaluated by CFD simulations. The effects of structure characteristics (width, number, and angular spacing of nozzles) on NO_x reduction and combustion performance were investigated in our research. Besides, the comparative analysis between the burner in operation and the optimized burner was also conducted in this study. The results gave a certain practical value for the combustion characteristics of the whole furnace.

Methodology

Research object

Figure 1(a) illustrates the schematic of the sidewall burner, which mainly includes the primary premixed gas inlet, secondary fuel gas, and air inlet. The primary premixed gas of the sidewall burner is mixed at the front-end of the ejector, then exits from the primary nozzle. Meanwhile, the secondary fuel gas and air are injected from secondary fuel gas nozzles and the air cylinder, respectively. The 3-D geometric model is also exhibited in fig. 1(b), and the cross-section of the burner built by SOLIDWORKS software is shown in fig. 1(c).

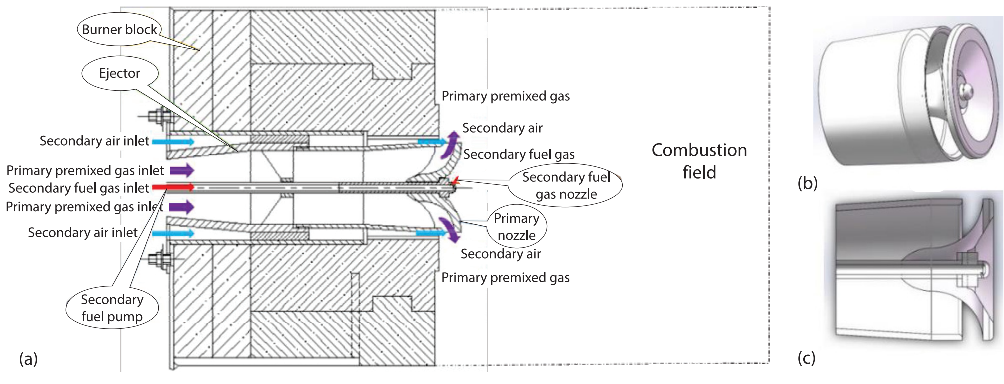

Figure 1. Configuration of sidewall burner; (a) schematic of the burner, (b) 3-D geometric model of the burner, and (c) cross-section of the burner

The main structural parameters of the sidewall burner in operation are listed in tab. 1. The width of the primary premixed gas outlet is 16 mm, the number of secondary fuel gas nozzles is 3, and the angular spacing of secondary fuel gas nozzles is 45°.

Table 1. The main structural parameters of the sidewall burner in operation

Items	Unit	Size
Primary premix length	mm	100
Maximum radius of the exit of the primary nozzle	mm	40
Exit angle of the primary nozzle	°	60
Length of the secondary fuel pipe	mm	117
Number of secondary fuel gas nozzles	–	3
Secondary fuel gas nozzle diameter	mm	1.6
Secondary fuel pipe diameter	mm	8
Angular spacing of secondary fuel gas nozzle	°	45
Width of the primary premixed gas outlet	mm	16

It was worth noting that a sidewall burner in operation furnace structure is used as the combustion field in numerical simulation evaluate the combustion performance. The furnace length of the sidewall burner is 325 mm, and the furnace diameter is set at 500 mm, which is taken as an example in the following simulation calculation.

Mesh

As shown in fig. 2, the grid was modelled by Pointwise software. Besides, the geometric model was divided into five parts, due to the relative complex construction of the sidewall burner, which could greatly improve the quality of the grid and the calculation efficiency. The figs. 2(a)-2(e) represent primary premixed pipeline fluid domain (a), secondary fuel injection fluid domain (b), air runner fluid domain (c), fuel line fluid domain (d), and furnace fluid domain (e), respectively. The components were assembled to form a complete computational fluid domain.

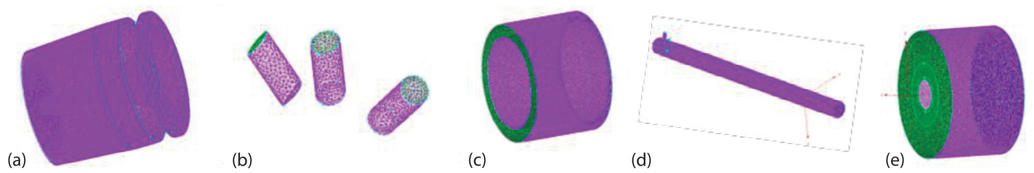

Figure 2. Integral grid of the fluid domain in the simplified model of the burner

In addition, in order to ensure the computational performance of the computational fluid domain, a grid independent test was also performed with the original burner. There different meshes were analyzed by NO_x emissions. The cell number of four meshes (Mesh 1, Mesh 2, Mesh 3 and Mesh 4) are 1.29×10^6, 3.28×10^6, 6.34×10^6, and 8.24×10^6, respectively. As shown in fig. 3, the solution of this case is independent of the grid size after the cell number is equal or greater than 3.28×10^6. Although the Meshes 3 and 4 need more computing resource than Mesh 2, it can provide more detailed in-flame information, which is important in this article. Moreover, the calculation results of Meshes 2-4 are similar. Therefore, the Mesh 2 was a balance between computing resource and grid quality, which was adopted in this study.

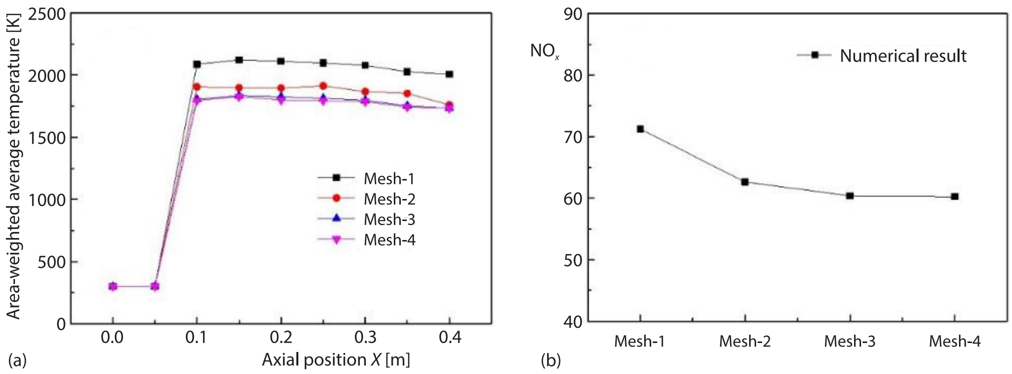

Figure 3. Integral grid of the fluid domain in the simplified model; (a) temperature and (b) NO_x

Description of the CFD method and boundary conditions

The CFD method

The FLUENT was used for this calculation. Using the realizable *k-ε* model for turbulence, the eddy dissipation concept (EDC) model for combustion, the discrete ordinates model for radiation, the JL-2 four-step reaction mechanism for methane, the five-step reaction mechanism for NO_x, and default parameters for model parameters.

Combustion mechanism: Based on the formation mechanism of NO_x, the emission of prompt NO_x was limited, which could be neglected [16]. Besides, the fuel gas was ideally considered as CH_4 (hereinafter referred to as fuel gas), and the fuel NO_x emission was limited in the combustion process [17]. That is, the thermal NO_x accounted for a large proportion of total NO_x emission, and, in this work, the NO_x formation was calculated based on the thermal NO_x.

In order to simplify the calculation, the JL-2 methane mechanism, the NO generation combined with the five-step reaction were applied in this work, and the mechanism of JL-2 methane could be calculated [18, 19]:

$$\mathrm{CH_4} + \frac{1}{2}\mathrm{O_2} \Rightarrow \mathrm{CO} + 2\mathrm{H_2} \tag{1}$$

$$\mathrm{CH_4} + \mathrm{H_2O} \Rightarrow \mathrm{CO} + 3\mathrm{H_2} \tag{2}$$

$$\mathrm{H_2} + \frac{1}{2}\mathrm{O_2} \Rightarrow \mathrm{H_2O} \tag{3}$$

$$\mathrm{CO} + \mathrm{H_2O} \Rightarrow \mathrm{CO_2} + \mathrm{H_2} \tag{4}$$

The reaction mechanism of NO_x was used by the overall package [20]:

$$\mathrm{N_2} + \mathrm{O_2} \Rightarrow 2\mathrm{NO} \tag{5}$$

Compared with the default two-step methane reaction and the NO_x reaction mechanism, the combustion mechanism used in this work made the numerical simulation calculation more reasonable.

Mathematical model: The mathematical model was vital in the numerical simulation calculation, which included the flow model, combustion model, and radiation model. These mathematical models were described in brief below. Turbulence flow was modelled by the realizable k-ε model, which introduced the items about rotation and curvature [21]. Since turbulence anisotropy was not significant, the realizable k-ε model was allowed in this numerical simulation calculation [22].

The EDC model was used. Using this model, the detailed chemical reaction mechanism in turbulent flow could be evaluated [23]. It has been found the EDC model was appropriate to calculate the process involved in the chemical-turbulence interaction [24, 25]. Besides, the EDC model could effectively reduce computational simulation time [26]. Thus, it was believed that the EDC model could be more suitable for simulating the burner. The radiative heat transfer of the mathematical model was modelled by the discrete ordinates model, which could meet the specular reflection or translucent situation [27].

Boundary conditions

The numerical simulation was carried out at the burner load of 0.337 MW, and the excess air coefficient was 1.1. In order to avoid a significant change in the density of flue gas due to change in the temperature and pressure, the mass-flow inlet was adopted for both fuel gas and air channel. The mass-flows of fuel gas and air were 0.0068 kg/s and 0.1787 kg/s, respectively. The boundary conditions, including the mass-flow rate, temperature, and hydraulic radius, were assumed as a uniform density distribution. The specific experimental settings were presented in tab. 2.

Table 2. Inlet boundary conditions of burner

Items	Mass-flow [kgs^{-1}]	Material composition	Mass fraction [–]	Inlet temperature [°C]	Inlet pressure [MPa]	Hydraulic diameter [m]
Primary gas mixture	0.0404	CH_4	0.11	25	0.13712	0.04
		O_2	0.21			
		N_2	0.68			
Secondary air	0.1429	O_2	0.23	25	0.101325	0.015
		N_2	0.77			
Secondary fuel gas	0.0021	CH_4	1.00	25	0.13712	0.002

The outlet boundary condition of the burner was determined as the outflow. Meanwhile, the hydraulic diameter calculation formula was calculated by eq. (6), where A represents the flow field and L represents the wetted perimeter:

$$D = \frac{4A}{L} \tag{6}$$

Model validation

For model validation, the calculated temperature at the outlet of the sidewall burner was compared to the experimental results. The portable thermocouples (SP30R, OMEGA, USA) were used to measure the area-weighted average temperature in experiments. As shown in fig. 4, the relative error between calculation and experiment is less than 10% at different burner loads

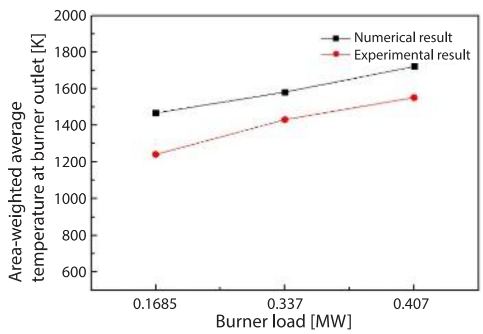

Figure 4. Numerical simulation and experimental temperature at the outlet of the sidewall burner

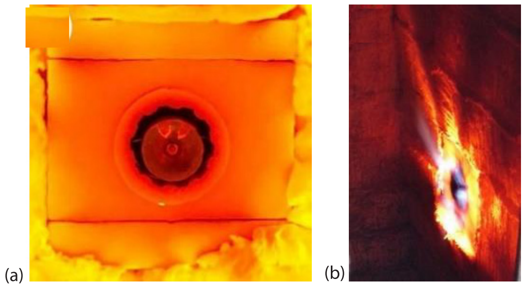

Figure 5. Combustion conditions of the sidewall burner in the furnace; (a) front and (b) side

(0.1685 MW, 0.337 MW, 0.407 MW). Although the temperature was measured by the uninsulated high precision thermocouple, the loss of heat through thermal radiation was unavoidable. However, the numerical study was conducted under adiabatic conditions. It was led to larger temperature deviations between the measured and calculated temperature values. That is, the actual temperature was higher than measured in the experiment and that is the reason why the relative error between calculation and experiment is 10%.

For further model validation, the NO_x emission was compared with experimental results. The flue gas analyzer (brain, 3040A, China) was used to measure the NO_x emission in experiments (61.11 ppm), and the relative error between calculation and experiment is less than 5%.

After the validation and comparison, it was concluded that the numerical model in this work is feasible and can be used for further investigation. Figure 5 describes the actual combustion conditions of the sidewall burner in the furnace.

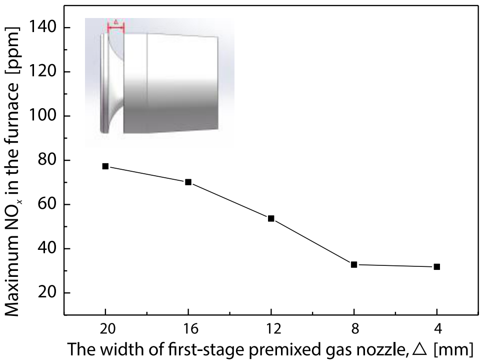

Figure 6. The NO_x emission at different primary premixed gas outlet widths

Results and discussion

Influence of the primary premixed gas nozzle structure on NO_x reduction and combustion performance

The width of the primary premixed gas outlet was a vital parameter for combustion, which was directly related to combustion performance. Figure 6 showed that the NO_x distributions at various primary premixed gas outlet widths Δ in the furnace. It could be observed that with the decrease of the primary premixed gas outlet width, the NO_x emission decreased from 77.2-53.6 ppm rapidly and then kept stable at 32 ppm.

This phenomenon could be explained by the following reasons. It was indicated that the fuel-air mixture had a significant effect on the temperature field and NO_x emission [28, 29]. Figure 7 showed that the temperature distributions at different gas outlet widths. It can be concluded that the decrease of the gas outlet width lead to the increase of velocity of the fluid. However, the high velocity of fluid may lead to backflow in the furnace, which has an adverse impact on combustion performance.

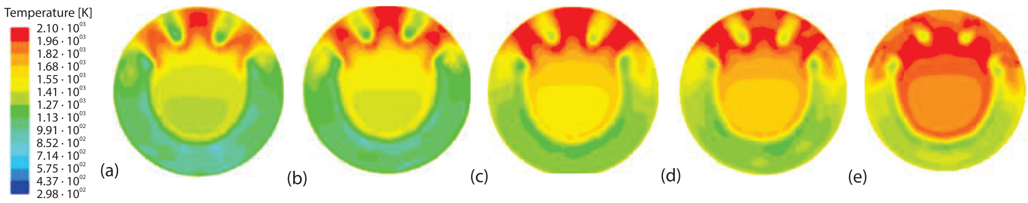

Figure 7. Temperature contours at different primary premixed gas outlet width (X = 0.2 m)

This result could also be explained by the contours of the CO concentration distribution along the horizontal plane of the furnace, as shown in fig. 8. According to the principle of the HC fuel combustion process, the shape of the flame could be reflected by the CO concentration approximately [30]. As shown in figs. 8(a)-8(d), the flame formed on both sides of the wall, and with the decrease of the width, the flame distribution became more uniform. However, when the primary premixed gas outlet width was more narrow, the fuel gas was affected by the backflow effect, resulting in the gathering in the center of the furnace. It should be noted that due to the structure of the sidewall burner, the concentration of the O_2 was insufficient in this zone. Therefore, the incomplete combustion situation was becoming more serious.

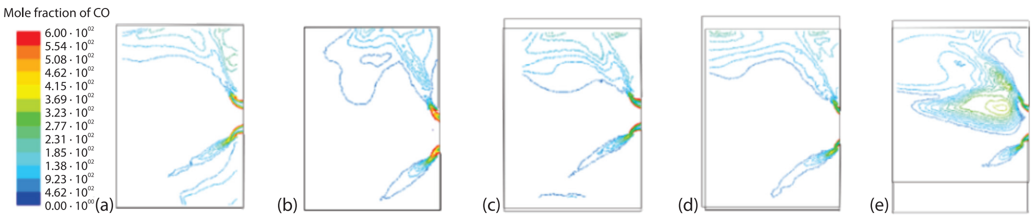

Figure 8. The CO concentration distribution at different primary premixed gas outlet width

Influence of secondary fuel gas nozzle structure on NO_x reduction and combustion performance

It was reported that the nozzle structure would change the fuel-air mixture, affecting the combustion performance [31]. The effect of the number of secondary fuel gas nozzles and angular spacing were investigated. The simulation was carried out at the boundary conditions shown in tab. 2.

Number of secondary fuel gas nozzles

The number of secondary fuel gas nozzles had an impact on the distribution of fuel in the furnace. It was necessary to investigate the influence of the number of secondary fuel gas nozzles. In simulation calculation, the number of nozzles was set at 1-5, respectively. The geometric model was shown in fig. 9.

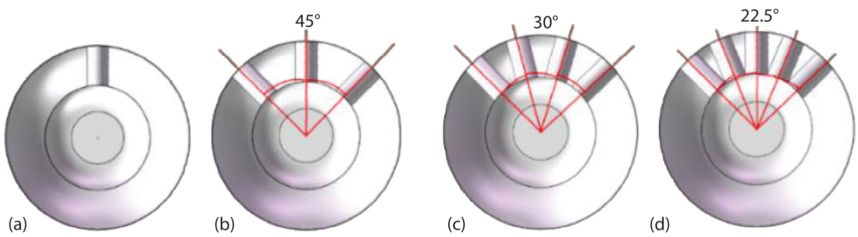

Figure 9. Geometric model of nozzles on the secondary fuel pump

The CH_4 concentration distribution was studied to evaluate the combustion characteristics. It could be observed from fig. 10 that the CH_4 injection distance decreased with the increase of the number of nozzles, which was ascribed to the reduction of partial pressure.

Figure 11 showed the concentration of CH_4 at different cross-sections. It can be found that the mass fraction of CH_4 dropped rapidly. Due to the consumption of CH_4, indicating that the combustion process was intensive in this field. However, the relatively low concentration of

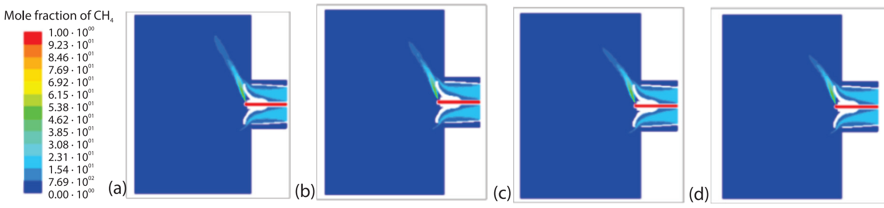

Figure 10. Mole fraction contours of CH_4 in the XZ plane

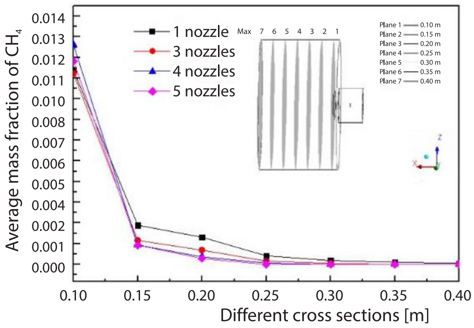

Figure 11. Average mass fraction of CH_4 at the different number of nozzles

CH_4 was observed from $x = 0.25$ to 0.4 m. It could be ascribed to the structure of the sidewall and the continuous combustion process.

The contours of temperature in the XZ plane were shown in fig. 12. It could be observed that the high temperature fields were mainly distributed in the upper part of the furnace. However, in the case of four nozzles, the smaller high temperature field was generated, indicating that a uniform distribution of fuel and air was provided, which might further decrease the NO_x emission [32, 33].

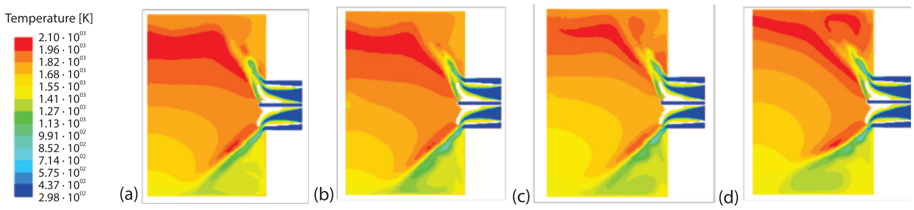

Figure 12. Temperature contours at the different numbers of nozzle

The NO_x and CO emission were shown in fig. 13. The results showed that the emissions of NO_x and CO were 28.8 ppm and 678 ppm in the case of 3 nozzles, respectively. The single nozzle showed a poor combustion condition, which generated 37.83 ppm of NO_x and 1189 ppm of CO. This result was mainly due to the incomplete combustion, causing by the lack of O_2 at the center of the furnace. More significantly, in the case of five nozzles, the lowest CO concentration could be achieved, indicating that the CH_4 and O_2 mixed well. The 5 nozzles case showed a relatively low velocity in the nozzles, leading to a longer residence time in the furnace and an increment of NO_x emission [34].

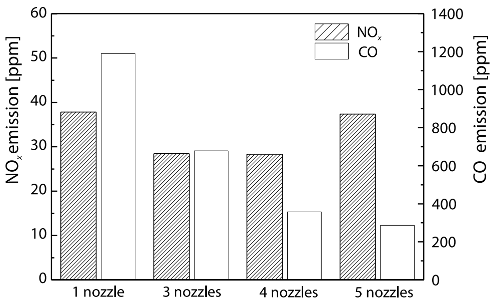

Figure 13. The NO_x and CO emission at different number of nozzles

Angular spacing of secondary fuel gas nozzles

The angular spacing of the secondary fuel gas nozzles was an important parameter that directly related to the fuel distribution. The effect of the angular spacing was investigated, and with the angular spacing changed from 30-60°, as shown in fig. 14.

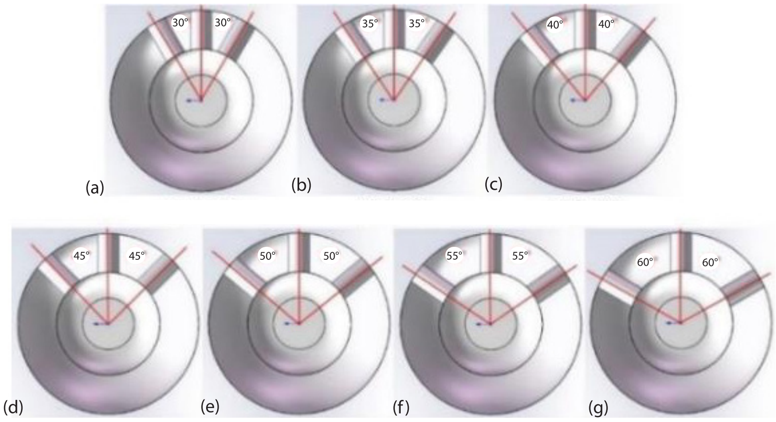

Figure 14. Geometric diagram of different nozzle angular spacing's

In order to evaluate the distribution of fuel gas, the contours of the mole fraction of CH_4 were shown in fig. 15. The angular spacing of the sidewall burner in operation was 45°, and the concentration of NO_x was 57.8 ppm in this condition. With the angular spacing increased from 30-60°, the distance between the directions of the fuel jets was increased, and the interference of jet fuels was weakened.

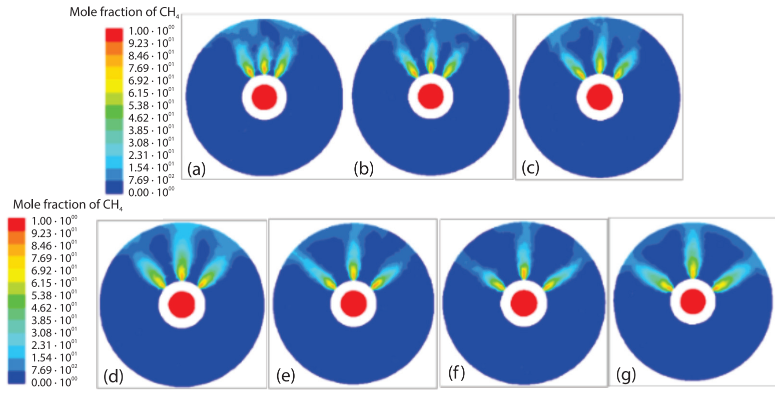

Figure 15. Mole fraction contour of CH_4 at different angular spacing's of nozzle

Figure 16 showed that the distribution of O_2 mass fraction with different nozzle angular spacings. It could be seen that the lowest O_2 mass fraction was obtained at the nozzle angular spacing of 55°, because of the distribution of O_2 on both sides of the primary premixed gas nozzle. The combustion process was sequentially improved together with the decline of NO_x emission.

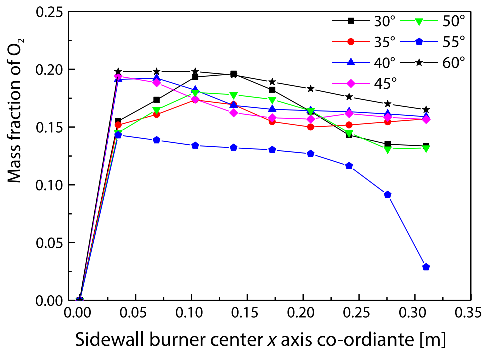

Figure 16. The distribution of O_2 mass fraction

As shown in fig. 17, the NO_x characteristics could be described by the contours of the NO_x distribution. It could be noted that with the angular spacing increased from 30-55°, the NO_x

emission decreased, while a slight increase was observed at an angular spacing of 60°. It could be explained by the following reasons. On the one hand, with the angular spacing increased, the negative pressure between nozzles reduced, leading to a decrease of O_2 concentration in this field. On the other hand, the O_2 concentration might have an impact on the combustion characteristics, and the lower NO$_x$ emission would be found with the longer angular spacing [35]. However, with the angular spacing further increased, it might cause the interference with an adjacent burner, which was not favourable for reducing emissions of NO$_x$.

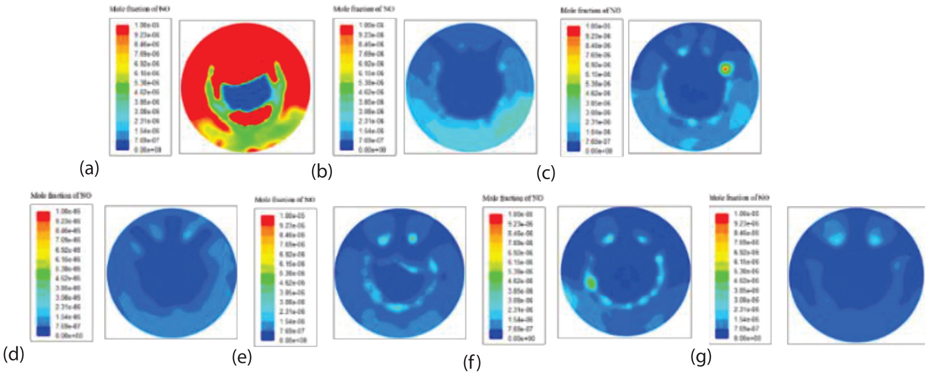

Figure 17. Mole fraction contour of NO$_x$ at different angular spacings θ (X = 0.2 m)

Conclusion

The structure of single low NO$_x$ burner involving width, number and the angular spacing of nozzle were optimized regarding the NO$_x$ reduction and combustion performance. The lowest NO$_x$ emission of 32.8 ppm was obtained at the width of 8 mm, while 28.33 ppm emission for NO$_x$ was achieved at the nozzle number of 4. The effect of the angular spacing of nozzles was firstly studied in the sidewall burner, showing that NO$_x$ emission was decreased with the increase of the angular spacing. The optimum angular spacing was 55° among the cases of 30°, 35°, 40°, 45°, 50°, and 60°.

Acknowledgment

This work was financially supported by International collaboration project from Department of Science and Technology of Jiangsu Province [Grant No. BZ2017014].

References

[1] Wang, Y. Q., *et al*., Experimental Investigation of the Characteristics of NO$_x$ Emissions with Multiple Deep Air-Staged Combustion of Lean Coal, *Fuel*, *280* (2020), 118416
[2] Abbasi, T., *et al*., Acid Rain: Past, Present, and Future, *International Journal of Environmental Engineering*, *5* (2013), 3, pp. 229-272
[3] Su, Y., *et al*., An Overview of Low NO$_x$ Gas Combustion Technology and Burner Design, *Industrial Boiler*, *4* (2016), pp. 17-25
[4] Houshfar, E., *et al*., Effect of Excess Air Ratio and Temperature on NO$_x$ Emission from Grate Combustion of Biomass in the Staged Air Combustion Scenario, Energy & Fuels, *25* (2011), 10, pp. 4643-4654
[5] Li, Z., *et al*., Combustion and NO$_x$ emission characteristics of a retrofitted down-fired 660 MWe utility boiler at different loads, *Applied Energy*, *88* (2011), 7, pp. 2400-2406
[6] Lee, C., *et al*., An Experimental Study on Industrial Boiler Burners Applied Low NO$_x$ Combustion Technologies, *Journal of Clean Energy Technologies*, *4* (2016), 6. pp. 430-434
[7] Gupta, A. K., *et al*., *Swirl Flow*s, Abacus Press, London, UK, 1984

[8] Nhan, H. K., *et al*., The CFD Investigation of NO_x Reduction with a Flue-Gas Internal Re-Circulation Burner in a Mid-Sized Boiler, *Journal of Mechanical ence and Technology*, *33* (2019), 6, pp. 2967-2978
[9] Chen, S., *et al*., The CFD Investigation on Low-NO_x Strategy of Folded Flame Pattern Based on Fuel-Staging Natural Gas Burner, *Applied Thermal Engineering*, *112* (2017), C, pp. 1487-1496
[10] Iyogun, C.O., *et al*., Experimental Investigation of the Effect of Fuel Nozzle Geometry on the Stability of a Swirling Non-Premixed Methane Flame, *Fuel*, *90* (2011), 4, pp. 1416-1423
[11] Fan, C., *et al*., Experimental Study of Sidewall Effect on Flame Characteristics of Heptane Pool Fires with Different Aspect Ratios and Orientations in a Channel, *Proceedings of the Combustion Institute*, *36* (2017), 2, pp. 3121-3129
[12] Eric, A., *et al*., Experimental and Numerical Study on Combustion of Baled Biomass in Cigar Burners and Effects of Flue Gas Re-Circulation, *Thermal Science*, *20* (2016), Suppl. 1, pp. S151-S165
[13] Guo, C., *et al*., Effect of Fuel Injection Characteristics on the Performance of a Free-Piston Diesel Engine Linear Generator: CFD Simulation and Experimental Results, *Energy Conversion and Management*, *160* (2018), Feb., pp. 302-312
[14] Khalilarya, S., Lotfiani, A.. Determination of Flow Pattern and Its Effect on NO_x Emission in a Tangentially Fired Single Chamber Square Furnace, *Thermal Scienc*e, *14* (2010), 2, pp. 493-503
[15] Goh, E., *et al*., Modelling of Minimum NO_x in Staged-Combustion Architectures at Elevated Temperatures, *Proceedings*, Asme Turbo Expo: Turbomachinery Technical Conference & Exposition, Charlotte, N. C. USA, 2017
[16] Alvarez, L., *et a*l., Oxy-Coal Combustion in an Entrained Flow Reactor: Application of Specific Char and Volatile Combustion and Radiation Models for Oxy-Firing Conditions, *Energ*y, *62* (2013), Dec., pp. 255-268
[17] Soete, G. G. D., Overall Reaction Rates of NO and N_2 Formation from Fuel Nitrogen, *Symposium on Combustion*, *15* (1975), 1, pp. 1093-1102
[18] Kim, J. P., *et al.*, Comparison of Different Global Reaction Mechanisms for Mild Combustion of Natural Gas, *Combustion Science and Technology*, *180* (2008), 4, pp. 565-592
[19] Novosselov, I. V., *et al.*, Development and Application of an Eight-Step Global Mechanism for CFD and CRN Simulations of Lean-Premixed Combustors, *Journal of Engineering for Gas Turbines & Power*, *130* (2008), 2, pp. 769-779
[20] Taniguchi, M., *et al*., Comparison of Staged Combustion Properties between Bituminous Coals and a Low-Rank Coal; Fiber-Shaped Crystallized Carbon Formation, NO_x Emission and Coal Burnout Properties at Very High Temperature, *Combustion & Flame*, *160* (2013), 10, pp. 2221-2230
[21] Shih, T. H., *et al*., A New Eddy k-ε Viscosity Model for High Reynolds Number Turbulent Flows, *Computer & Fluids*, *24* (1995), 3, pp. 227-238
[22] Jovanovic, R., *et al*., Experimental and Numerical Investigation of Flame Characteristics During Swirl Burner Operation under Conventional and Oxy-Fuel Conditions, *Thermal Science*, *21* (2017), 3, pp. 1463-1477
[23] Farokhi, M., Birouk, M., A New EDC Approach for Modelling Turbulence/Chemistry Interaction of the Gas-Phase of Biomass Combustion, *Fuel*, *220* (2018), May, pp. 420-436
[24] Lupant, D., Lybaert, P., Assessment of the EDC Combustion Model in MILD Conditions with in-Furnace Experimental Data, *Applied Thermal Engineering*, *75* (2015), Jan., pp. 93-102
[25] Garcia, A. M., *et al*., Combustion Model Evaluation in a CFD Simulation of a Radiant-Tube Burner, *Fuel*, *276* (2020), 118013
[26] Vaid, H. S., *et al.*, A Run Time Combustion Zoning Technique Towards the EDC Approach in Large-Scale CFD Simulations, *International Journal of Numerical Methods for Heat & Fluid-flow, 24* (2013), 1, pp. 21-35
[27] Habibi, A., *et al.*, Multiscale Modelling of Turbulent Combustion and NO_x Emission in Steam Crackers, *AIChE Journal, 53* (2010), 9, pp. 2384-2398
[28] Bulysova, L. A., *et al.*, Parametric Computational Studies of NO_x Emission Reduction in Staged Combustion of Ideal Fuel-Air Mixtures, *Power Technology and Engineering 52* (2018), 2, pp. 1-7
[29] Terasaki, T., *et al.*, The Effects of Fuel-Air Mixing on NO*x* Formation in Non-Premixed Swirl Burners, *Symposium on Combustion, 26* (1996), 2, pp. 2733-2739
[30] Cuoci, A., *et al.*, The Ignition, Combustion and Flame Structure of Carbon Monoxide/Hydrogen Mixtures, Note 2: Fluid Dynamics and Kinetic Aspects of Syngas Combustion, *International Journal of Hydrogen Energy, 32* (2007), 15, pp. 3486-3500
[31] Yang, X., *et al.*, Numerical Investigation on the Mixing Process in a Steam Ejector with Different Nozzle Structures, *International Journal of Thermal Sciences, 56* (2013), June, pp. 95-106

[32] Fu, Z., *et al.*, Generation Characteristics of Thermal NO_x in a Double-Swirler Annular Combustor under Various Inlet Conditions, *Energy, 200* (2020), 117487
[33] Schluckner, C., *et al.*, Fast and Accurate CFD-Model for NO_x Emission Prediction During Oxy-Fuel Combustion of Natural Gas Using Detailed Chemical Kinetics, *Fuel, 264* (2020), 15, 116841
[34] Chen, H., *et al.*, Combustion and NO_x Emission Behavior of Chinese Coals, *Chinese Journal of Chemical Engineering, 10* (2002), 3, pp. 333-338
[35] Yan, Y., *et al.*, Influence of Oxygen Concentration on Combustion Characteristics of Inferior Coal and Sludge Mixture, *Journal of Fuel Chemistry and Technology, 41* (2013), 4, pp. 430-435

Paper submitted: September 16, 2020
Paper revised: December 1, 2020
Paper accepted: December 3, 2020